Universiteit
Leiden
The Netherlands

Probing spatial heterogeneity in supercooled glycerol and temporal heterogeneity with single-molecule FRET in polyprolines

Xia, T.

Citation
Xia, T. (2010, March 25). *Probing spatial heterogeneity in supercooled glycerol and temporal heterogeneity with single-molecule FRET in polyprolines*. *Casimir PhD Series*. Retrieved from https://hdl.handle.net/1887/15122

Version:	Corrected Publisher's Version
License:	Licence agreement concerning inclusion of doctoral thesis in the Institutional Repository of the University of Leiden
Downloaded from:	https://hdl.handle.net/1887/15122

Note: To cite this publication please use the final published version (if applicable).

2 Soft glassy rheology of supercooled liquids

Abstract – We probe the mechanical response of two supercooled liquids, glycerol and *ortho*-terphenyl, by conducting rheological experiments at very weak stresses. We find a complex fluid behavior suggesting the gradual emergence of an extended, delicate solid-like network in both materials in the supercooled state, i.e., *above* the glass transition. This network stiffens as it ages, and very early in this process it already extends over macroscopic distances, conferring all well-known features of soft glassy rheology (yield-stress, shear thinning, aging) to the supercooled liquids. Such viscoelastic behavior of supercooled molecular glass formers has not been reported before; our results suggest this is because the large stresses in conventional rheology can easily shear-melt the solid-like structure. The work presented here, combined with evidence for long-lived heterogeneity from previous single-molecule studies [Zondervan R, Kulzer F, Berkhout GCG, Orrit M (2007) "Local viscosity of supercooled glycerol near T_g probed by rotational diffusion of ensembles and single dye molecules", *Proc Natl Acad Sci USA* 104:12628–12633], has a profound impact on the understanding of the glass transition, since it casts doubt on the widely accepted assumption of the preservation of ergodicity in the supercooled state.

The contents of this chapter have been published:
R. Zondervan, T. Xia, H. van der Meer, C. Storm, F. Kulzer, W. van Saarloos, and M. Orrit, *Proc. Natl. Acad. Sci. USA* **105** (2008) 4993–4998.

2.1 Introduction

Many liquids fail to crystallize when they are cooled below their thermodynamic solidification temperature (the melting point of the crystal). Instead, these supercooled liquids become enormously viscous, eventually turning into solid glasses when their glass-transition temperature T_g is reached. After more than half a century of research, the structural glass transition remains mysterious [47]. It has long been clear that glass formation requires cooperation beyond the molecular scale [4], and is intimately connected with inhomogeneities. The nature, length-scale and timescale of these inhomogeneities are unknown. One may envision them as frozen-in density fluctuations. They cause deviations from pure liquid behavior, and tend to relax by processes known as environmental exchanges. The exchange timescales must be significantly longer than those of the pure liquid. If they exceed experimental times, ergodicity is broken in practice, and the system appears heterogeneous.

Heterogeneity is readily observed in optical experiments on supercooled liquids, notably in light and X-ray scattering [11, 12], polarized hole-burning [13, 14], single-molecule spectroscopy [15, 16], and it appears to relax slowly. Tracking of individual particles in colloidal glasses [48,49], as well as computer simulations [50–52], provides further evidence for heterogeneity, and confirms that relaxation is driven by collective rearrangements. In parallel, a large body of experimental data [4] from molecular-scale techniques – most importantly NMR [7, 8] and dielectric relaxation [9, 10] spectroscopy – also suggests dynamical heterogeneity, with a length scale that increases upon approaching the glass transition temperature [53]. The latter experiments, however, invariably find relaxation time scales comparable to molecular reorientation times (α-relaxation), and length scales of a few nanometers only.

Our group has recently studied the local relaxation of supercooled glycerol, up to 30 K above its glass transition, using single-molecule polarization microscopy [1]. The rotational dynamics of individual chromophores provides a nanometer-scale probe of the material in which they are embedded. These experiments showed that different single dye molecules tumble at different rates in the supercooled glycerol in which they are dissolved, with the spread of tumbling times spanning almost one decade. Our most surprising observation was that environmental exchanges were very rare, even over the several hours of a typical measurement. This period is up to about one million times longer than the α-relaxation time, i. e., the average tumbling time of a glycerol molecule [1]. It is very difficult to reconcile such long exchange times with the picture of a pure liquid, in which all molecules should be equivalent on average. It was therefore suggested [1] that the long memory arises from nearly static

structures, which form a fragile solid-like network dividing the supercooled liquid into heterogeneous "liquid pockets." Such a scenario naturally explains our previous single-molecule experiments, as well as similar studies in another molecular glass former, *ortho*-terphenyl (OTP) [15]. However, the existence of such static structures is completely at odds with the commonly-held view of supercooled liquids above the rheological glass transition, in which fast environmental exchanges are thought to quickly erase memory effects, and to restore ergodicity. We therefore performed the rheological experiments reported here to test our hypothesis of the presence of an extended solid-like network in supercooled molecular liquids. As it turned out, we indeed found surprising behavior for both supercooled glycerol and OTP.
An embedded solid network can be expected to lead to non-Newtonian rheology, a behavior that is actually the rule in heterogeneous fluid mixtures, gels, suspensions, emulsions, foams, slurries, pastes, quicksand, and surprisingly even in simple fluids close to the critical point [54]. All these systems display distinctly non-liquid-like characteristics such as viscoelasticity, yield stress, shear-thinning, and aging – a combination of features known as "soft glassy rheology" [55]. Similar properties have furthermore been reported in simulations of Lennard–Jones glasses [56]. For the present investigation we chose two archetypal molecular glass formers which were previously studied by single-molecule microscopy [1, 15]: glycerol ($T_\mathrm{g} = 190\,\mathrm{K}$), which is a comparatively strong glass former due to its extended network of hydrogen bonds, and *ortho*-terphenyl (OTP, $T_\mathrm{g} = 244\,\mathrm{K}$), whose structure is governed by weaker van der Waals interactions. We indeed find pronounced non-Newtonian behavior, which manifests itself significantly above the glass transition temperature for both of these materials, and we thus demonstrate for the first time that supercooled molecular liquids can exhibit all the hallmarks of soft glassy rheology. The history-dependent behavior shows that such molecular glass formers already exhibit clear signatures of non-ergodic behavior in a significant temperature range above the glass transition temperature.

2.2 Experimental methods

2.2.1 Sample preparation

Anhydrous glycerol (specified to contain less than 0.1 % water) was used as obtained from Sigma-Aldrich, transferred from the newly-opened bottle into the Couette cell (see Figure 2.7) as quickly as possible and then purged repeatedly with dry helium gas. *Ortho*-terphenyl *purissimum* (Fluka, purity greater than 99 %) was distilled twice before usage. All rheological samples were kept

under a dry helium atmosphere for the duration of the experiments.

2.2.2 Design of the Couette cell

The rheology experiments were conducted with a variable-temperature Couette cell (see Figure 2.7), in which a sample film filled the gap between an inner cylinder and an outer cup. Torque was applied to the cylinder by means of a torsional spring and the viscoelastic response of the sample was deduced from the subsequent movement of the cylinder, which was recorded via the deflection of a laser beam. Additional experimental details can be found in the appendix.

2.3 Results

2.3.1 Viscoelastic behavior and yield stress

Previous studies of the viscosity of glycerol [57] and OTP [58] throughout the supercooled region down to their respective glass transition temperatures failed to find deviations from Newtonian behavior (apart from the expected observation of viscoelasticity at high frequencies). However, the putative solid-like network is thought to be formed only very slowly, and by limited inhomogeneous compaction of the liquid - not by extended homogeneous crystallization. Therefore we can expect this network to break or shear-melt at the comparatively large stresses ($> 1\,\mathrm{MPa}$ [57]) that are used in conventional viscosity measurements. Accordingly, we have built a temperature-variable Couette cell that allowed us to apply weak stresses. Furthermore, since the rheological response in yield-stress materials can be highly nonlinear, we did not follow the usual approach of recording the harmonic response with sinusoidal excitation. Instead, in order to discriminate easily between liquid and yield-stress behavior, we applied constant torques (see Experimental methods section and the appendix for details).
We found that both glycerol and OTP continued to behave as seemingly perfect Newtonian liquids during the initial cooldown - even for the smallest stress we could apply ($\approx 100\,\mathrm{Pa}$), and all the way down to a few Kelvin above their respective glass transition temperatures. The measured viscosities were in agreement with those previously reported (as can be seen in Figure 2.5 in the appendix). However, the emergence of solid-like behavior could be observed in both materials when the temperature was raised again after a significant waiting period, as shown in Figure 2.1.

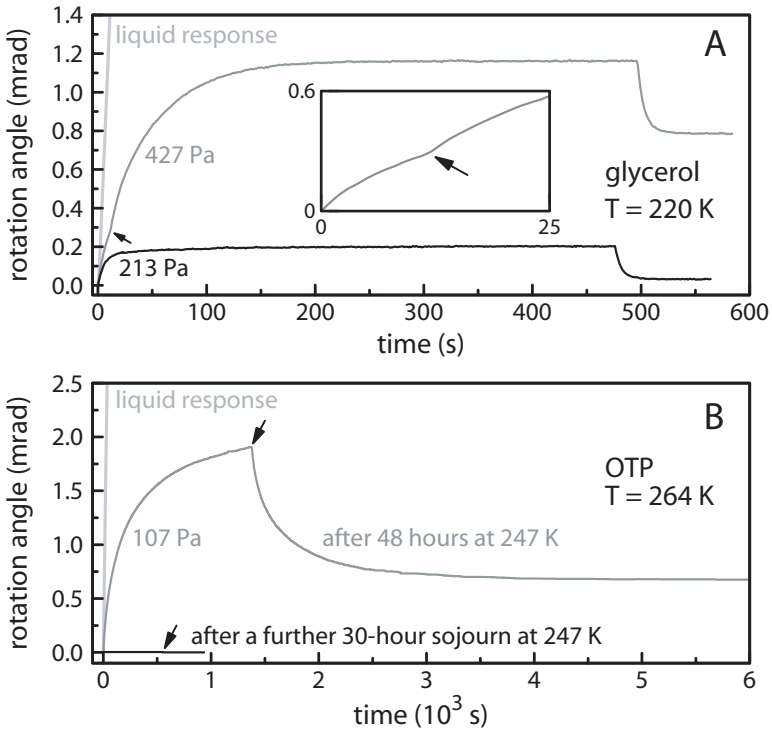

Figure 2.1: Viscoelastic behavior of supercooled glycerol and OTP. (A) Shear strain response of supercooled glycerol at 220 K, induced by the application of a constant shear stress at time zero. The plot shows the liquid-like reaction during the initial cooldown (light gray line, at 213 Pa shear stress) and the viscoelastic behavior that could be observed after an excursion to 197 K = T_g + 7 K (black curve at 213 Pa, gray curve at 427 Pa). In the case of the latter two curves the torque was released at about 470 s, giving rise to a backward spring motion toward the initial position. The data for 427 Pa exhibits a yielding event (marked by an arrow, see also the enlarged view in the inset) and the initial position is not recovered. (B) Shear strain response of supercooled OTP, measured at 264 K for an applied shear stress of 107 Pa, at three different stages of aging. The light gray line shows the liquid-like response observed during initial cooldown. After 48 hours at 247 K (T_g + 3 K), a clear solid-like response appeared (gray curve). The system sprang back toward its initial position after removal of the applied shear stress (denoted by the arrow). The associated shear modulus was about 10 kPa, 100,000 times smaller than the shear modulus of crystalline OTP. After the next excursion to 247 K (30 hours) the system had become so hard that no response could be measured at 264 K, even at the largest stress we could apply (3 kPa). The associated shear modulus was greater than 10 MPa.

In the case of glycerol, we allowed for aging periods of about one hour at 197 K ($T_g + 7$ K) and then the material was brought to 220 K. We chose this probing temperature for practical reasons; testing flow properties took only a few minutes at 220 K, whereas reaching the same deformation at a given applied torque would have required 130 times longer at 205 K and 4000 times longer at 197 K. We then repeated this cooling/warming cycle a few times (see Figure 2.6 and accompanying text in the appendix), until a clear solid-like behavior appeared: Upon application of the shearing torque, the angle of the inner cylinder reached a quasi-stationary value (see Figure 2.1 A), which then continued to drift slowly. This observation is the signature of a solid-like connection between the inner Couette cylinder and the outer cup. For larger torques, breaking events occurred at a shear deformation around $0.1 - 0.2$ %, as the bottom trace in Figure 2.1 A shows, and the rotation angle did not return to its initial value when the stress was released. This points to the expected yield-stress, and confirms the considerable nonlinearity of the mechanical properties of the supercooled liquid in this regime, already for low stresses (200 Pa) and small deformations (about 0.1 %). Breaking events may arise from shear localization, as found earlier in numerical simulations of glasses [56].
We used the same experimental protocol for OTP, adjusting the parameters to allow for the higher glass transition temperature of OTP ($T_g = 244$ K) and for the differences in viscosity, which affect the kinetics of the formation of the solid network. Consequently, we cooled the OTP sample down to 247 K, 3 K above the glass transition temperature. After 48 hours at 247 K, the temperature was raised to 264 K within about one hour, and the mechanical properties were tested. Already after less than one hour waiting time at 264 K, the material exhibited a very clear solid-like response, as shown in Figure 2.1 B. As was the case with glycerol, we found that once the solid response had appeared, the system continued aging and became increasingly stiff, at a rate that strongly depended on temperature. This behavior is very similar to that reported for OTP by Patkowski et al. [11,12], who detected the scattering signature of a "supercooled liquid with clusters."

2.3.2 Phenomenological model

To evaluate the angular traces quantitatively, we fitted them with a simple phenomenological model (see Figure 2.2 A). We think of the aged supercooled liquid as a solid-like network that responds elastically for small deformations, and which is embedded in a viscous fluid. A movement of the inner cylinder in the Couette cell gives rise to two torques: a viscous one from the surrounding

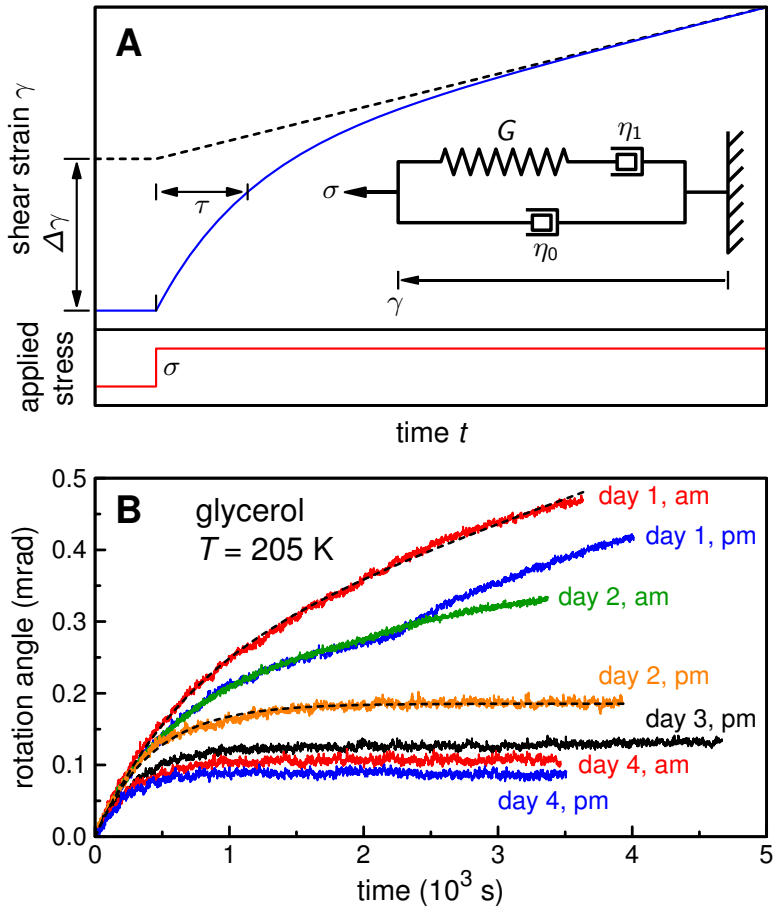

Figure 2.2: Rheological response of a solid-like network which is embedded in a liquid. (A) Phenomenological model for the quantitative evaluation of rotation traces, from which three parameters are deduced: the shear modulus G of the solid network, the viscosity η_0 of the embedding liquid, and the effective viscosity η_1 representing plastic deformation of the solid network. The constant shear stress σ is suddenly applied at time zero. The expression of the characteristic time τ is given in the text and the strain amplitude $\Delta\gamma$ is the prefactor of the exponential term in Eq. (2.1). (B) Examples of strain traces acquired during the aging and hardening of glycerol, induced by the application of a constant shear stress $\sigma = 107\,\mathrm{Pa}$ at time $t = 0$. The plot shows data taken during the first 4 days of an observation period of 2 weeks. The traces were fitted with Eq. (2.1) resulting from the model described in (A), except when breaking events occurred (e.g., day 1, pm). The dashed lines give two examples of these fits to the data.

fluid, and an (initially) elastic one from the solid network. The solid network will soon undergo microscopic rearrangements and will yield for large enough deformation. We represent this plastic deformation as another viscous response. As a first-order approximation, we neglect a possible strong dependence of this effective viscosity on the applied stress (see next section, Figure 2.4). We therefore represent the solid network as a spring and a dashpot in series (adding deformations), and this viscoelastic system itself is placed in parallel (adding torques) with a dashpot representing the liquid, as shown in Figure 2.2 A. In the spirit of a mean-field approximation, we consider the whole system as a collection of identical cells, all of them with the same elastic modulus and effective viscosities. This oversimplified model obviously fails to represent individual breaking events. The shear strain response $\gamma(t)$ of the model to a constant stress σ applied at time zero is easily found to be a superposition of a linear drift in a fluid with a total effective viscosity $\eta = \eta_0 + \eta_1$ (the sum of the viscosity η_0 of the liquid and of the effective viscosity η_1 of the network), and of an exponential transient:

$$\gamma(t) = \frac{\sigma}{\eta_0 + \eta_1}\, t + \frac{\sigma}{G} \left(\frac{\eta_1}{\eta_0 + \eta_1} \right)^2 \left\{ 1 - \exp\left(-\frac{t}{\tau} \right) \right\} \quad . \tag{2.1}$$

The latter term corresponds to stretching the springs of the solid-like network, represented by the shear rigidity modulus G, in the surrounding liquid; this process has a characteristic response time τ:

$$\tau = \frac{1}{G}\, \frac{\eta_0\, \eta_1}{\eta_0 + \eta_1} \quad . \tag{2.2}$$

Fitting the experimental trajectories with this model gave us the three rheological parameters of the material, η_0, η_1, and G at every temperature and any stage of the aging process. Some examples of fitted traces are shown for glycerol in Figure 2.2 B. We then followed the aging of glycerol at the constant temperature of 205 K for more than two weeks. The evolution of the three parameters G, η_0, and η_1 during this period is presented in Figure 2.3 A. The effective viscosity η_1 was often difficult to determine at later stages of the aging process, because experimental drifts overwhelmed the weak creep signal. Moreover, η_1 strongly depended on the applied torque. We nevertheless indicate several values of η_1 in Figure 2.3 A to give a feeling for the large increase of effective viscosity correlated with the increase in stiffness of the network. In contrast, the viscosity η_0 was found to be constant within experimental error, and consistent with the viscosity of supercooled glycerol obtained in previous rheological measurements [57]. This result suggests that the solid network remained a minor component of the fluid throughout our study of Figure 2.3 A.

The most remarkable feature is the large increase of the shear rigidity modulus G, by two orders of magnitude over two weeks at 205 K. At the end of this measurement run, the shear modulus had reached about 1 MPa, a value that is, however, still more than three orders of magnitude lower than the modulus of crystalline glycerol [59].
Similarly, we followed the rheological response of the OTP sample as it aged over a period of more than two weeks at a temperature of 256 K. The three parameters G, η_0, and η_1 were again fitted using the model described in Figure 2.2; these data are shown in Figure 2.3 B. As with glycerol, the liquid viscosity η_0 of OTP was comparable to the literature value and to our measurement of the viscosity of the non-aged sample at that temperature (about 10 MPa·s). We again found a pronounced stiffening: The shear modulus increased by more than two orders of magnitude in about 14 days, and did not yet seem to saturate at the end of the measurement. However, the maximum value of about 10 MPa is still two orders of magnitude smaller than the shear modulus of crystalline OTP. The measurements were stopped at that point because, at the maximal torque we could apply, the accuracy of our rheometer was not sufficient to measure smaller deformations.

2.3.3 Shear thinning and rejuvenation

We have seen that, when left undisturbed, supercooled glycerol hardens over time, but it shows shear-thinning when strongly perturbed. Figure 2.4 A presents a different run of aging experiments, again indicating hardening at 205 K for days $1-4$. On day 5, we applied large shears to the sample (more than 10 times the shear previously used for probing) for several minutes. After this strong perturbation, the material presented a liquid-like response with a large amplitude, indicating that the solid connection had been disrupted, possibly by shear banding. This trace was very similar to that of day 1, illustrating the phenomenon of rejuvenation by a strong strain (such shear rejuvenation phenomena are currently attracting interest in other complex fluids as well [60,61]). Nevertheless, if the system is left unperturbed, the solid connection can heal quickly; in our case the hardening process had resumed already during the night between days 5 and 6. Due to experimental limitations in the applied torques, we could not test if the memory of previous aging can be erased permanently by sufficiently energetic stirring.
Figure 2.4 B documents another manifestation of shear thinning. The apparent (total) viscosity of the material during the first waiting period at 197 K after the first cooldown is measured by the long-time drift of the inner cylinder under an applied torque. If the torque is increased, the apparent viscosity

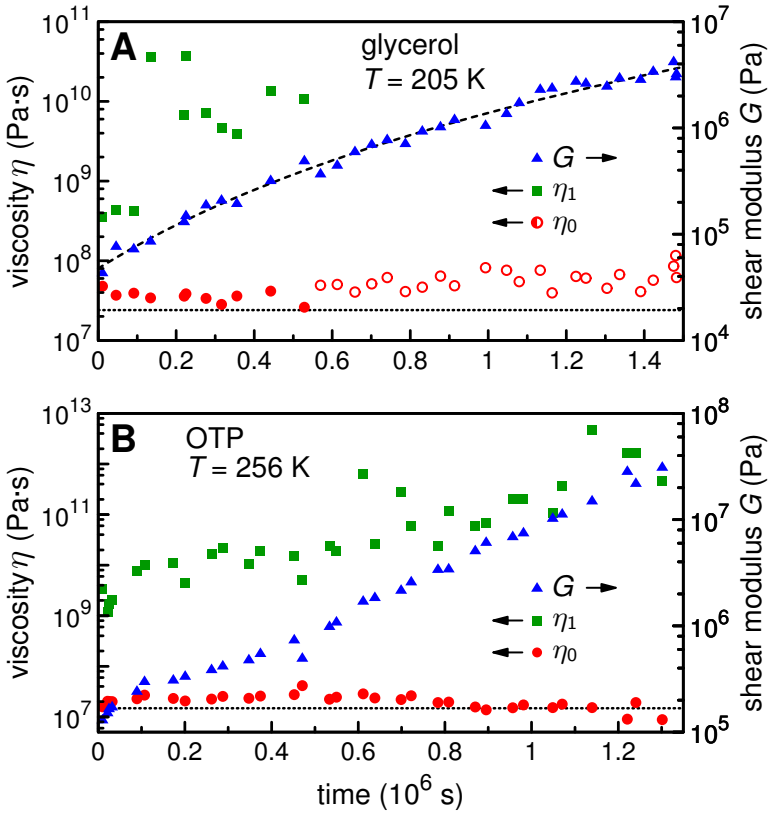

Figure 2.3: Aging of glycerol and OTP. (A) Aging of the shear modulus G (right y-axis) and of the viscosity parameters η_0 and η_1 (left y-axis) of glycerol at 205 K as a function of time over a period of two weeks. Note that the system already presented a weak shear modulus at the beginning of the measurements. The values of the effective viscosity η_1 (squares) depend on the applied stress (see Figure 2.4). The measurements up to 0.5 Ms were done at a shear stress of 107 Pa (filled circles representing η_0), later measurements at 213 Pa and 427 Pa (open circles). The dotted line corresponds to the viscosity derived from the liquid response at large stress, which is close to the literature value. The dashed curve, drawn through the shear modulus data points (triangles) as a guide to the eye, is a fit by a power law of time, $G(\mathrm{Pa}) = 10^{-18.5} \times [t(\mathrm{s}) + 750,000]^{3.9}$. (B) Aging of OTP over a period of two weeks at 256 K. The plot shows the evolution of the viscosities η_0 (circles, left y-axis) and η_1 (squares, left y-axis), as well as of the shear modulus G (triangles, right y-axis). The dotted line denotes the viscosity value derived from the liquid response during initial cooldown, which is in agreement with previous measurements.

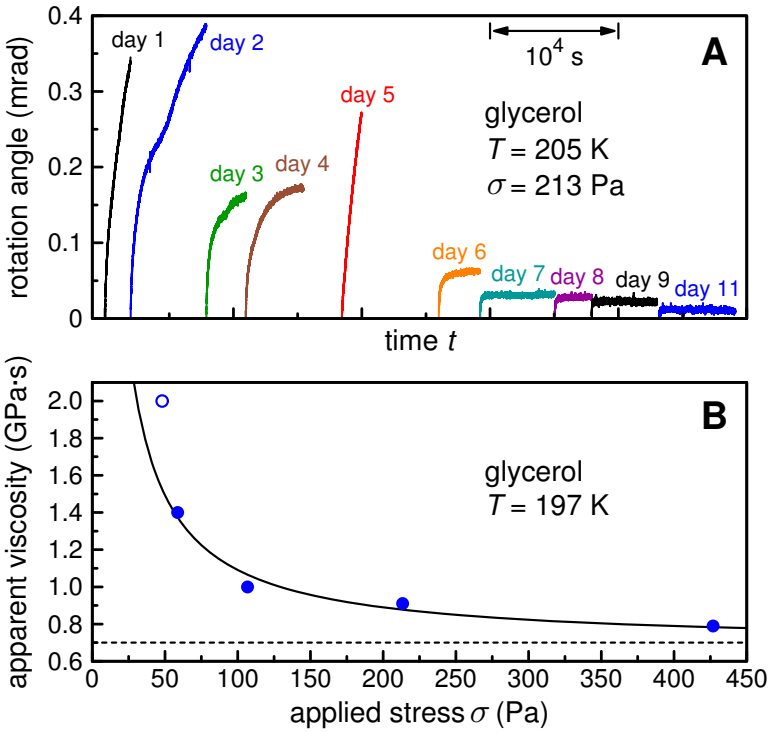

Figure 2.4: Shear thinning and rejuvenation of supercooled glycerol. (A) Hardening of glycerol at 205 K, which is interrupted by temporary rejuvenation due to the application of a large shear stress (day 5). (B) Shear thinning at 197 K due to the application of increasingly larger torques.

decreases. We can provide a first-order description of this effect with the following mean-field model: Consider a typical hydrogen bond in the solid network, and suppose that this bond can break under stress or under thermal fluctuations and can also reform with rate k_r, possibly at a different place. According to Kramers' theory of passage of an activation barrier [62], the rate of bond opening k_o is modified by the application of an external force F according to:

$$k_\mathrm{o}(F) = K \exp\left(\frac{a\,F}{k_\mathrm{B}\,T}\right) \equiv K \exp\left(\frac{F}{F_0}\right) \quad , \tag{2.3}$$

where a is a characteristic bond length, k_B is the Boltzmann constant, and K is the rate in the limit of $F \to 0$. Upon deformation of the solid network, an average force develops from stretching the network's springs represented by

the shear-modulus G. This force acts only during the periods when the bond is closed. The average force, proportional to the deformation rate $\dot{\gamma}$, can be represented by an effective viscosity η_1:

$$\eta_1(F) = \frac{1}{2} \frac{G}{k_\mathrm{o}(F)} \frac{k_\mathrm{r}}{k_\mathrm{r} + k_\mathrm{o}(F)} \quad , \tag{2.4}$$

which decreases exponentially with the applied force. However, we have to realize that the force F that acts on the solid network (see the model described in Figure 2.2 A) is not exactly the applied total force F_t. The difference arises because the network is yielding and there is an additional viscous force from the liquid component. According to the model, F and F_t are indeed related by:

$$F = \frac{\eta_1}{\eta_0 + \eta_1} F_\mathrm{t} \quad . \tag{2.5}$$

In this expression, the viscosity η_1 itself depends on the force F according to Eq. (2.4). Together, Eqs. (2.4) and (2.5) lead to an implicit equation for the effective viscosity. The exact solution of these equations for forces much larger than $k_\mathrm{B}T/a$ shows that the effective viscosity varies approximately as $1/F_\mathrm{t}$, i.e., much slower than the exponential decay of Eq. (2.3). This approximation has been used to fit the experimental data in Figure 2.4 B (filled circles). It correctly predicts an asymptotic approach to the viscosity of the liquid for a large applied force (dashed line, value taken from Ref. [57]) and a slow algebraic decay of the effective viscosity (the data point for the lowest torque, i. e., the open circle in Figure 2.4 B, is less reliable, being close to our instrumental limit. This point has therefore been disregarded in the fit).

2.4 Discussion

The crucial feature of our experiments is that, once supercooled glycerol and OTP have been kept for some time at temperatures slightly above the glass transition, they show a combination of liquid- and solid-like behaviors: Our force response measurements reveal that, in addition to the expected viscous response, there is a small elastic component whose strength increases steadily with time. The typical shear rigidities that we found were considerably smaller than those of the crystalline materials: the shear rigidity modulus always stayed at least three orders of magnitude below that of the crystal for glycerol, and two orders of magnitude for OTP. We could measure such weak shear rigidities, because we allowed the systems to age and then perturbed them only weakly and rarely. Presumably, in typical viscosity measurements

with conventional oscillatory rheometers, a delicate solid-like network is either shear-melted or prevented from forming altogether. We have been able to shear-melt the network by subjecting it to sufficiently large torques. Their initial fragility explains why such solid-like structures have not been reported earlier.

Observing these signatures of a solid-like network in the macroscopic properties of these glass formers is in agreement with the evidence for long-lived structural heterogeneity on the microscopic scale. Previous studies of single molecules embedded in supercooled OTP [15] and glycerol [1] reported that the probe chromophores locally experience a liquid environment, but that they display a large spread in individual correlation times. The environment of each individual molecule appeared static over time scales that are long compared to both the rotational correlation time of the probe and the α-relaxation time of the host. This effect was most dramatic for glycerol, with the memory time being at least five orders of magnitude greater than the rotational correlation time of the dye and more than a million times longer than the α-relaxation time of glycerol. The combined experimental evidence on microscopic and macroscopic scales inevitably leads one to conclude that, after a temperature quench to a few degrees *above* T_g, supercooled molecular liquids can develop a fragile solid-like elastic matrix that encloses liquid pockets. This scenario was proposed earlier to explain the aforementioned single-molecule results [1]; it is completely consistent with the rheological measurements presented here. The picture that thus emerges is that a supercooled molecular liquid can phase-separate into locally liquid and solid-like regions, leading to the emergence of solid-like yield stresses and elastic moduli, which build up over temperature-dependent time scales. As conjectured earlier [63], we find that a supercooled liquid can exhibit soft glassy rheology well above T_g, and that the onset of this rheological behavior coincides with the appearance of structural heterogeneity, reminiscent of that found in computer simulations [64] and colloids [48], but associated here with such an extreme separation of scales that ergodicity is effectively broken tens of degrees above the glass transition temperature.

While phase separation is normally characterized by ever-increasing length scales as the domains of each phase coarsen, this apparently is not the case in the systems we investigated. A natural interpretation of this observation is in terms of frustration – either a geometric frustration as proposed by Tarjus *et al.* [65], a dynamic frustration, or both. Such frustration limits the size that domains can attain, and, in an equilibrium system, can indeed lead to an "avoided critical point". In practice, dynamical arrest will most likely be important: It is natural to assume, and consistent with light scattering, that

the two phases will have different densities. Therefore, any mass transport required for phase separation will be prohibitively slowed down due to the high viscosity and reduced pore size. This scenario indeed agrees with our observation that the aging of the network (which we infer from its increasing shear modulus) proceeds slower at lower temperatures. In this scenario, the previously reported broad distribution of single-molecule rotational diffusion times [1, 15] reflects the differences in densities in the various liquid pockets, as well as, possibly, the pocket size.[1] The ratio $D\eta/T$ should be constant if the Stokes–Einstein relation holds, but is found to increase sharply as one approaches the glass point [66]. This increase is naturally explained by the large dispersion of local viscosities. The average mobility determination of D is biased toward the fastest molecules in the low-viscosity liquid lakes, whereas the average viscosity favors the slowest molecules in the high-viscosity lakes [66]. With solid-like parts, this difference between the two averages becomes extreme. This description is similar to Bouchaud's concept of self-inhibitory dynamics in glasses and granular materials [67], in which an important ingredient is the postulated local conservation of free volume. Free volume conservation would naturally follow from an effective sealing of local areas by a solid-like structure. A related picture is provided by the defect-diffusion model of Shlesinger and colleagues [68], according to which different amounts of free volume can be trapped in different mobility islands. In first approximation, we can relate the concentration of free volume in each island to a local pressure. From the change of the average viscosity with pressure [69] and the spread in local viscosity uncovered in the single-molecule measurements [1], we can estimate the variation of the local pressure to be about $1 - 2\,\mathrm{bar}$ for glycerol. Neither the typical scale nor the short-range structure of the solid-like network can be determined directly from our present experimental results. However, the above picture implies long-lived density fluctuations, which should be visible in light scattering experiments. Indeed, a large excess of Rayleigh-scattered compared to Brillouin-scattered light has been observed in the spectra of OTP [12, 70] and other molecular glass formers. Ultrasmall-angle X-ray scattering [11] indicates the presence of slowly-relaxing density fluctuations on even smaller scales. The combined evidence from all these experiments

[1] Corrections to the rotational diffusion coefficient of a particle a distance r from a wall fall off as r^{-3} due to hydrodynamic interactions. For a confined molecule, this leads to a correction in the diffusion coefficient of the order $a(S/V)$, where a is the molecular size, and S/V the surface to volume ratio of the confining volume. In the absence of density differences, this would allow one to extract a distribution of pockets sizes from the observed distribution of rotational diffusion times. Presumably, however, the density corrections dominated in our previous single-molecule experiments [1].

points to a broad range of scales for the density inhomogeneities, from about ten to at least a few hundreds of nanometers, with extremely slow relaxation – up to a million times slower than α-relaxation processes. Furthermore, the excess light scattering depends on the thermal history of the sample, similar to what we observe for the viscoelastic response. (Careful sample preparation and handling can produce specimens in which the excess light scattering is absent or in which its occurrence is significantly delayed [12].) While these light scattering results are thus largely consistent with our measurements (which probe both smaller and larger length scales), their interpretation in terms of isolated clusters in a liquid phase [11,12,70,71] is not supported by the gradual build-up of a finite shear rigidity that we observe. Instead, our results imply the existence of a continuous, system-spanning network [72] that ages over time, as was discussed above. Future study of more supercooled liquids will show whether this feature is generic for molecular glass-formers, or even for glasses in general.

It is noteworthy that extrapolation of the spread in tumbling times of our single-molecule data to higher temperatures suggests that the heterogeneity of the liquid pockets disappears at a temperature somewhat below $1.2\,T_\mathrm{g}$ [1]. In other words, this type of behavior is found roughly in the same temperature range $T_\mathrm{g} < T < 1.2\,T_\mathrm{g}$ in which fragile glasses are known to show strong non-Arrhenius behavior. One has to wonder whether this is just a coincidence, or the signature of a characteristic property of the supercooled state. In addition to exploring this behavior systematically as a function of temperature and aging for various materials, an important issue for future research is therefore whether the rheological anomalies studied would fail to appear or to grow above some temperature around $1.2\,T_\mathrm{g}$. Furthermore, these findings may also clarify a puzzling feature of mode-coupling theory (MCT), its prediction of a sharp transition to a non-ergodic kinetically arrested phase at a critical temperature T_c significantly larger than T_g, sometimes called the "best-known failure" of MCT [73]. Our experiments suggest that this supposed failure may only reflect the inadequacy of the widely assumed ergodicity and uniqueness of the metastable supercooled liquid above T_g. They suggest that the main problem may lie in the association of T_c with T_g. Our results show that both supercooled glycerol and supercooled OTP can exhibit all the features commonly found in the soft glassy rheology of a complex fluid: flow, rigidity, yield stress, aging, rejuvenation and shear melting. Rather than either flow or break, these supercooled liquids actually flow and break at the same time, and they do so already at temperatures significantly above their respective glass transition temperatures.

Acknowledgements

We thank H. S. Overkleeft and A. M. C. H. van den Nieuwendijk for help with the distillation of OTP. This work is part of the research program of the "Stichting voor Fundamenteel Onderzoek der Materie" (FOM), financially supported by NWO.

2.5 Appendix

2.5.1 Viscosities of glycerol and *o*-terphenyl

The plots in Figure 2.5 show measurements of the viscosities of glycerol and OTP in the temperature range of interest. The filled circles represent experiments that were conducted with our rheometer during initial cooldown, when both substances exhibited purely liquid-like behavior. The solid lines correspond to literature data measured by the drop method for glycerol [57] and by conventional rheology as well as by the beam-deformation method for OTP [58]. The agreement is very good for glycerol. For OTP, our measurements seem to slightly overestimate the viscosity by a factor of about 1.5, most probably due to systematic differences in the determination of the absolute temperature or other calibration effects. Nevertheless, the temperature dependence of the measured values is in very good agreement with the published data.

2.5.2 Onset of solid-like behavior in glycerol

An overview of the thermal history of the glycerol sample used in the rheology experiments is given in Figure 2.6. Each individual trace starts at or above room-temperature with an initial overnight cooldown (at a rate of about 5 K/hour) and presents the subsequent temperature variations with time until we observed the onset of a solid-like behavior. The first detection of a shear modulus at 220 K is indicated by the squares which terminate the curves. From that point on we lowered the temperature to 205 K for the aging study presented in Figures 2.3 and 2.4.
The chronological order of the traces in Figure 2.6 is from bottom (oldest) to top (newest) and reflects how we gradually homed in on experimental temperature profiles leading to a solid-like behavior. The thermal history of our previous single-molecule experiments [1] also shows a long period (about 6 days) at 195 K, close to the glass transition, followed by warming up to 205 – 215 K, when the single molecules were measured. (These studies were con-

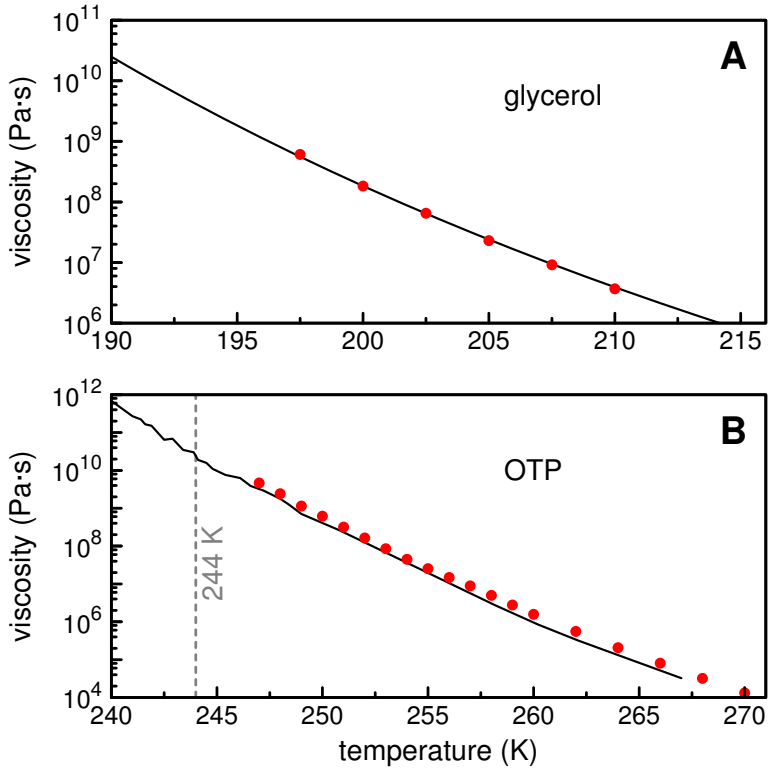

Figure 2.5: (A) The viscosity of glycerol ($T_g = 190\,\mathrm{K}$) as a function of temperature. The solid line represents reference data taken from the literature [57], the circles show the results of our measurements of the liquid response. (B) The viscosity of OTP ($T_g = 244\,\mathrm{K}$) as a function of temperature (circles: our measurements during the initial cooldown; curve: reference data [58]).

ducted several months before the rheology experiments.) Comparison to the traces for bulk glycerol strongly suggests that the extended network was also present in the single-molecule sample at the time the temperature-dependent experiments were performed.

The conclusion of this preliminary study is that the growth of the solid network is initiated after a ripening period of at least a few hours at 197 K, 7 K above the nominal glass transition. Note, however, that a more sensitive probing of elastic properties of the supercooled liquid could perhaps detect the onset of the solid network at earlier stages still. Furthermore, it can be expected that single-molecule measurements already reveal structural heterogeneity long before the solid network has become extended enough to influence the mechanical

properties of a bulk sample. This suggests that a more sensitive probing of the early stages in the development of the solid-like network is possible in future experiments with individual chromophores.

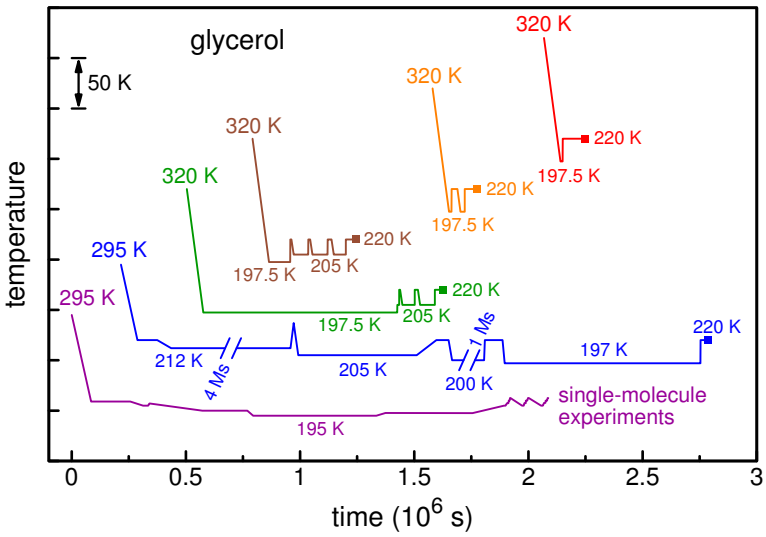

Figure 2.6: The thermal history of the glycerol sample in our rheological studies. Each trace is terminated by a square which indicates the first detection of solid-like behavior. The thermal history of the sample in our previous single-molecule experiments [1] is included for comparison (bottom trace).

2.5.3 Experimental details

Design of the Couette Cell. The design of our rheometer is shown schematically in Figure 2.7. A home-built Couette cell was integrated into a variable-temperature cryostat (Janis SVT-200-5). A film of glycerol or OTP, respectively, with a thickness of two millimeters resided between a movable inner cylinder and a static outer cup. Adjustable torque could be applied with a load lever on top of the cryostat via a bronze wire that acted as a torsional spring. The resulting movement of the inner cylinder was inferred from the deflection of a helium-neon laser beam which was retro-reflected by two mirrors rigidly connected to the cylinder and the cup, respectively. This arrangement, with the two mirrors (initially) perpendicular to each other, helps to ensure that the direction of the reflected laser beam is sensitive only to the motion of the inner cylinder relative to the outer cup. The difference signal of a split photodetector was used as an error indicator to control a galvanometer mirror.

The current fed into the galvanometer mirror was adjusted by a servo loop to compensate for rotation of the inner cylinder, and therefore provided a direct measure for its rotation. The sensitivity limit of the apparatus was found to correspond to a relative deformation of about 5×10^{-5}.

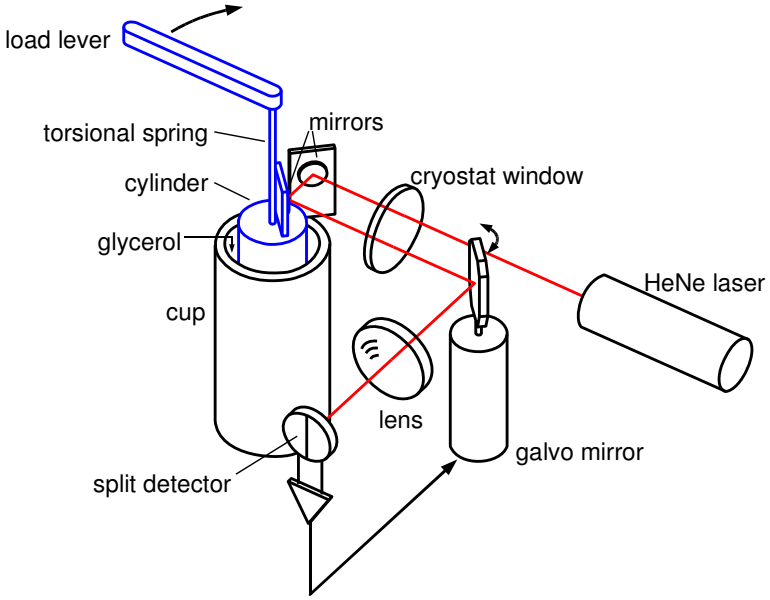

Figure 2.7: Schematic drawing of the Couette cell.

Calculation of Shear Modulus and Viscosity. The (quasi-)static values of the shear modulus G and of the viscosity η relate the elastic stress σ_{el} and the viscous stress σ_{visc} to the strain γ and the shear-rate $\dot{\gamma}$ by:

$$\sigma_{\mathrm{el}} = G\,\gamma \qquad \text{and} \qquad \sigma_{\mathrm{visc}} = \eta\,\dot{\gamma} \quad . \tag{2.6}$$

The stress and strain are related to the applied torque M and the rotation angle θ of the inner cylinder according to:

$$\gamma = \frac{R\,\theta}{d} \qquad \text{and} \qquad \sigma = \frac{M}{2\pi\,R^2\,h} \quad . \tag{2.7}$$

The geometrical characteristics of the cell are the average cylinder radius R, the height h of glycerol between the cylinders, and the glycerol film thickness

d. We can now relate the intrinsic properties G and η of the material to the experimental parameters:

$$\eta = C\,\frac{M}{\dot{\theta}} \qquad \text{and} \qquad G = C\frac{M}{\theta} \qquad \text{with} \qquad C = \frac{d}{2\pi\,R^3\,h} \quad . \tag{2.8}$$

The torsion constant of the wire, 0.0767 Nm/rad, which is needed to relate the applied torque to the twist angle of the wire, was determined at room-temperature by incorporating the wire into a torsion pendulum and measuring the oscillation period of a known, variable moment of inertia.
Because of the slight rotation of the inner cylinder, the torque produced by the torsion wire was not kept exactly constant during the deformation. However, the maximum rotation angle of the inner cylinder was very small compared to the twist angle of the wire, less than 0.7 % for the weakest shear moduli in Figure 2.3. Even for the qualitative demonstration of the solid-like behavior of OTP (gray trace in Figure 2.1B), the deformation remained below 10 % of the applied twist angle. Therefore, to a good approximation, the applied torque can be considered as constant during each individual measurement.
The smallest shear stress that could be applied reproducibly was about 55 Pa. Conducting control experiments under these conditions to check for the presence of solid friction in our apparatus, we could not detect any friction effects above our sensitivity limit.